

Adult Bone Marrow–derived Cells Do Not Acquire Functional Attributes of Cardiomyocytes When Transplanted into Peri-infarct Myocardium

John A Scherschel^{1,2}, Mark H Soonpaa^{1,2}, Edward F Srouf^{1,3,4}, Loren J Field^{1,2} and Michael Rubart¹

¹Department of Pediatrics, Division of Cardiology, Wells Center for Pediatric Research, Indianapolis, Indiana, USA; ²Department of Medicine, Division of Cardiology, Krannert Institute of Cardiology, Indiana University School of Medicine, Indianapolis, Indiana, USA; ³Department of Medicine, Division of Hematology/Oncology, Indiana University School of Medicine, Indianapolis, Indiana, USA; ⁴Department of Microbiology/Immunology, Indiana University School of Medicine, Indianapolis, Indiana, USA

The cardiomyogenic potential of adult bone marrow (BM) cells after being directly transplanted into the ischemically injured heart remains a controversial issue. In this study, we investigated the ability of transplanted BM cells to develop intracellular calcium ($[Ca^{2+}]_i$) transients in response to membrane depolarization *in situ*. Low-density mononuclear (LDM) BM cells, c-kit-enriched (c-kit^{enr}) BM cells, and highly enriched lin⁻ c-kit⁺ BM cells were obtained from adult transgenic mice ubiquitously expressing enhanced green fluorescent protein (EGFP), and injected into peri-infarct myocardiums of nontransgenic mice. After 9–10 days the mice were killed, and the hearts were removed, perfused in Langendorff mode, loaded with the calcium-sensitive fluorophore rhod-2, and subjected to two-photon laser scanning fluorescence microscopy (TPLSM) to monitor action potential–induced $[Ca^{2+}]_i$ transients in EGFP-expressing donor-derived cells and non-expressing host cardiomyocytes. Whereas spontaneous and electrically evoked $[Ca^{2+}]_i$ transients were found to occur synchronously in host cardiomyocytes along the graft–host border and in areas remote from the infarct, they were absent in all of the >3,000 imaged BM-derived cells that were located in clusters throughout the infarct scar or peri-infarct zone. We conclude that engrafted BM-derived cells lack attributes of functioning cardiomyocytes, calling into question the concept that adult BM cells can give rise to substantive cardiomyocyte regeneration within the infarcted heart.

Received 2 February 2008; accepted 5 March 2008; published online 22 April 2008. doi:10.1038/mt.2008.64

INTRODUCTION

Conflicting data exist as to the ability of adult bone marrow (BM) cells to give rise to cardiomyocytes within the injured heart.¹ The possibility of cardiomyocyte formation by adult BM-derived stem cells was initially demonstrated in a study by Bittner *et al.*,² who observed dystrophin-expressing cardiomyocytes in *mdx* mice after BM reconstitution with wild-type donor cells. Subsequently,

Jackson *et al.*³ induced myocardial ischemia/reperfusion injury in mice after BM reconstitution with so-called side population cells that were genetically engineered to express β -galactosidase. Donor cell–derived cardiomyocytes were detected in the peri-infarct zone, albeit at a very low prevalence (0.02%). A study by Xaymardan *et al.*⁴ showed that a small percentage of fluorescently labeled unfractionated BM cells obtained from adult rats can acquire a cardiomyocyte phenotype in an infarct transplantation model. Similarly, fluorescently tagged BM mononuclear cells from patients with previous myocardial infarction were shown to transdifferentiate into cardiomyocytes when seeded on cryoinjured mouse ventricles in culture.⁵

A limited number of studies have reported extensive myocardial regeneration from BM-derived cells within the infarcted heart.^{6,7} In these latter studies, female mice were subjected to permanent coronary artery ligation, and c-kit-positive BM cells from adult male transgenic mice ubiquitously expressing enhanced green fluorescent protein (EGFP) were directly injected into the viable peri-infarct region. *De novo* formation of donor cell–derived cardiomyocytes was assessed by co-staining for cardiomyocyte-specific markers plus Y chromosome or EGFP. By this approach, it was demonstrated that transplanted BM cells could give rise to millions of new cardiomyocytes by 9 days after intracardiac injection, resulting in partial replacement of the scar with functioning muscle. The concomitant improvement of left ventricular contractility led the authors to suggest that *de novo* cardiomyocytes became electromechanically integrated and were thus capable of directly contributing to the overall pump function of the injured heart.

Numerous other studies have failed to observe cardiomyogenic differentiation from adult BM-derived donor cells. For example, Balsam *et al.*⁸ demonstrated that purified populations of adult hematopoietic stem cells obtained from transgenic mice widely expressing EGFP transiently engrafted within the infarcted myocardium, but did not express cardiac tissue–specific markers. Rather, most of the donor-derived cells expressed the pan-hematopoietic marker CD45 and the myeloid marker Gr-1. Nygren *et al.*⁹ did not observe cardiomyogenic transformation of unfractionated BM cells or c-kit⁺-enriched hematopoietic stem

Correspondence: Michael Rubart, Wells Center for Pediatric Research, 1044 West Walnut Street, Indianapolis, Indiana 46202, USA.
E-mail: mrubartv@iupui.edu

cells after engraftment within the infarcted mouse myocardium, as evidenced by the absence of cardiomyocyte-specific immune reactivity in the donor cells. Murry *et al.*¹⁰ utilized cardiomyocyte-restricted transgenes (expressing either β -galactosidase or EGFP under the regulation of the α -cardiac myosin heavy chain promoter) as well as a ubiquitously expressed EGFP reporter transgene (in conjunction with histochemical analyses) to track the fate of two purified populations of BM-derived hematopoietic stem cells ($\text{lin}^- \text{c-kit}^+$ and $\text{lin}^- \text{c-kit}^+ \text{sca-1}^+$ cells) after their transplantation into injured hearts. Although donor cells did engraft in the damaged muscle, no transdifferentiation events were detected, as evidenced by the lack of expression of a cardiomyocyte-restricted reporter transgene, as well as the absence of cardiomyocyte-specific immune reactivity in the donor cells.¹⁰

When all these findings are considered collectively, the question of whether regeneration of cardiomyocytes can be achieved by engrafting adult BM-derived cells within the injured heart remains highly controversial, despite the use of seemingly identical donor cells and experimental conditions in various studies. In this study, we elected to use an assay that relied on examination of function rather than of potentially subjective immune histologic endpoints, to examine the regenerative potential of adult BM-derived cells in the infarcted heart. Specifically, we systematically probed the ability of engrafted BM-derived cells to develop intracellular calcium ($[\text{Ca}^{2+}]_i$) transients in response to membrane depolarization within the intact heart, using a previously developed two-photon laser scanning microscopy (TPLSM)-based imaging technique.^{11,12} A side-by-side comparison was performed, of low-density mononuclear (LDM) BM cells, c-kit-enriched ($\text{c-kit}^{\text{enr}}$) BM cells, and highly enriched hematopoietic stem cells ($\text{lin}^- \text{c-kit}^+$ BM cells), obtained from adult transgenic mice ubiquitously expressing EGFP. We demonstrate that all donor cell types were efficiently engrafted in the infarcted tissue of nontransgenic recipient hearts at day 9 after the cell injection. However, while spontaneous and electrical stimulation-induced $[\text{Ca}^{2+}]_i$ transients were observed to occur synchronously in host cardiomyocytes along the graft–host border, they were absent in all of the >3,000 imaged BM-derived cells that were located in clusters within the infarct scar or border zone. These results indicate that engrafted BM-derived cells lack fundamental attributes of functioning cardiomyocytes, and further call into question the concept that adult BM cells can give rise to substantive cardiomyocyte regeneration within the infarcted heart.

RESULTS

Donor cell preparation

ACT-EGFP mice were used for isolating donor BM cells. These mice express EGFP under the control of the chicken β -actin promoter.¹³ In control experiments, a comparison of 10- μm sections obtained from adult *ACT-EGFP* and wild-type mouse hearts under epifluorescence illumination demonstrated that all cardiomyocytes in the transgenic hearts expressed EGFP throughout the cytoplasm and nuclei (Figure 1). The kinetics of electrically evoked $[\text{Ca}^{2+}]_i$ transients in adult *ACT-EGFP* hearts were indistinguishable from those in wild-type hearts (data not shown). From these observations, we expect any BM-derived cardiomyocytes

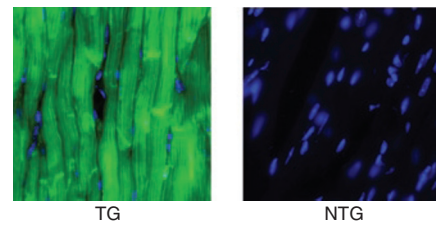


Figure 1 Representative epifluorescence images of 10- μm sections obtained from the hearts of an adult *ACT-EGFP* transgenic (TG) mouse and its nontransgenic (NTG) adult littermate. Sections were stained with Hoechst. Images for EGFP (green) and Hoechst (blue) fluorescence were merged. The imaging parameters were identical for both sections. EGFP, enhanced green fluorescent protein.

from *ACT-EGFP* mice to express EGFP stably, and to function normally.

Three different donor BM cell populations were studied, namely, LDM BM cells, c-kit-enriched ($\text{c-kit}^{\text{enr}}$) BM cells, and highly enriched lineage negative (lin^-) c-kit⁺ BM cells. LDM BM cells were isolated using a density centrifugation protocol as published earlier.⁹ $\text{c-kit}^{\text{enr}}$ BM cells were isolated using magnet-activated cell sorting. Flow cytometry analyses of the $\text{c-kit}^{\text{enr}}$ BM cells demonstrated that the percentage of c-kit-positive cells in the eluted (*i.e.*, labeled) fraction from the magnetic column was approximately fivefold to sixfold larger than that in the eluent (*i.e.*, unlabeled) fraction (Figure 2a). The $\text{c-kit}^{\text{enr}}$ BM cell population was further assayed for the expression of EGFP and a variety of surface antigens. Before enrichment, 35% (dotted area in Figure 2b) of the cells in the initial LDM BM preparation were EGFP positive (Figure 2c). We confirmed the percentage of EGFP-expressing cells using additional epifluorescence analyses. Our number is in good agreement with earlier studies that used EGFP reporter transgenes to track the cardiomyogenic potential of marrow-derived cells.^{7,14} $\text{c-kit}^{\text{enr}}$ BM cells were 45% negative for a cocktail of antibodies that recognize mature hematopoietic cells, including lymphocytes, monocytes, granulocytes, neutrophils, and erythrocytes (Figure 2d). Markers for hematopoietic stem and progenitor cells (CD34, sca-1, flk-1) were present in 4% (flk-1) to 21% (sca-1) of the $\text{c-kit}^{\text{enr}}$ BM cell population (Figure 2e–g). Restricting the flow cytometry analysis to the subfraction of EGFP-positive cells within the $\text{c-kit}^{\text{enr}}$ BM cell population did not alter the expression profile of surface antigens (see Supplementary Figure S1), thereby suggesting that the presence of the fluorescent protein does not impart negative or positive selections on BM subpopulations. Highly enriched $\text{lin}^- \text{c-kit}^+$ BM cells were prepared by first removing cells expressing hematopoietic lineage markers through magnetic immunobead subtraction.¹⁵ This lin^- fraction was then reacted with an anti-c-kit monoclonal antibody and separated using fluorescence-activated cell sorting into c-kit^+ and c-kit^- cells (Figure 2h). Lin^- cells that showed c-kit expression levels 2-fold to 100-fold higher than EGFP⁻/ c-kit^- cells were used for intracardiac transplantation (only EGFP-expressing cells were used).

ACT-EGFP BM-derived cells stably engraft infarcted myocardium

The peri-infarct regions of nontransgenic hearts were injected with 100,000 LDM, $\text{c-kit}^{\text{enr}}$, or $\text{lin}^- \text{c-kit}^+$ BM cells. The mice were

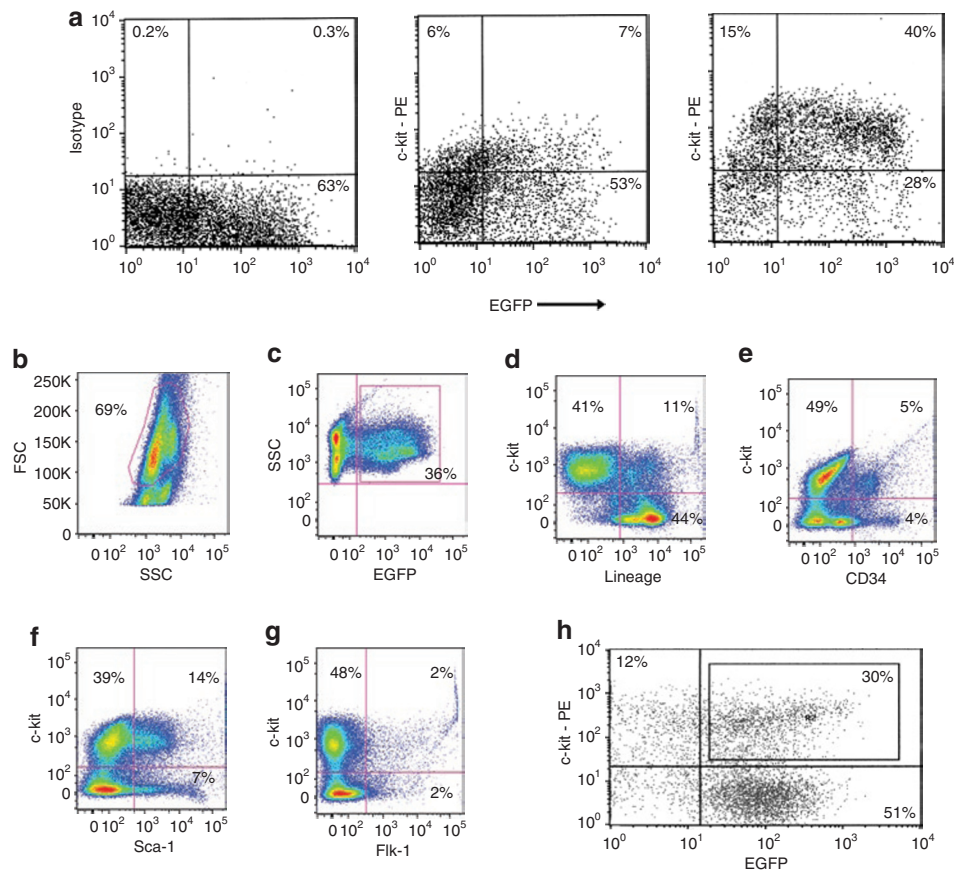


Figure 2 Analysis of $c\text{-kit}^{\text{enr}}$ (panels **a–g**) and highly enriched $\text{lin}^- c\text{-kit}^+$ (panel **h**) bone marrow (BM) cells. **(a)** Representative flow cytometry dot plots of the eluted (positively labeled; right panel) and eluent (unlabeled; middle panel) fractions of $c\text{-kit}^{\text{enr}}$ BM cells based on levels of enhanced green fluorescent protein (EGFP) (x -axis) and $c\text{-kit}$ (y -axis) expressions. The left panel shows isotype control. The axes are log-scaled. **(b–g)** Flow cytometry analyses of surface antigen expression in $ACT\text{-EGFP } c\text{-kit}^{\text{enr}}$ BM cells. $c\text{-kit}^{\text{enr}}$ BM cells were selected for $c\text{-kit}^+$ ($CD117^+$) cells using magnet-activated cell sorting as described in Materials and Methods. **(b)** Light scatter gating of eluted cells identified ~70% of the cells within the low-density mononuclear gate (FSC, forward scatter). **(c)** Analysis of GFP expression versus side scatter (SSC) identified 35% of eluted cells as GFP^+ . **(d)** Expression of lineage markers (x -axis) versus $c\text{-kit}$ expression (y -axis) among cells falling within the mononuclear gate as defined in **b**. **(e)** Expression of CD34 (x -axis) versus $c\text{-kit}$ expression (y -axis) among cells falling within the lymphocyte gate. **(f)** Expression of Sca-1 (x -axis) versus $c\text{-kit}$ expression (y -axis) among cells falling within the mononuclear gate. **(g)** Expression of Flk-1 (x -axis) versus $c\text{-kit}$ expression (y -axis) among cells falling within the mononuclear gate. **(h)** Fluorescence-activated cell sorting (FACS) of $ACT\text{-EGFP}$, lineage-depleted (lin^-) mouse BM cells based on $c\text{-kit}$ and EGFP expression. Representative FACS dot plot of lin^- BM cells stained with ACK-4/Biotin/streptavidin–phycoerythrin (streptavidin–PE). Antibody-labeled cells were separated using FACS into four subsets based on the number of $c\text{-kit}$ receptors (y -axis) and levels of EGFP (x -axis) expression. The box in upper right rectangle indicates the fraction of $c\text{-kit}^+/EGFP^+$ cells that was used for cell transplantation ($\text{lin}^- c\text{-kit}^+$ group). The mean expression levels of both $c\text{-kit}$ and EGFP in $c\text{-kit}^+/EGFP^+$ cells were ~2-fold to ~100-fold higher than those in $c\text{-kit}^-/EGFP^-$ cells (lower left rectangle).

subsequently killed and the hearts were removed and processed to monitor scar formation and donor cell viability, using sirius red/fast green histochemical staining and a chromogenic anti-EGFP immune reactivity assay, respectively. The analysis was performed at 9 to 10 days after the engraftment, because earlier studies had suggested that extensive cardiomyocyte regeneration from $\text{lin}^- c\text{-kit}^+$ BM cells takes place within this period.^{6,7,16} **Figure 3** shows representative examples of grafts generated with each cell type. In accordance with earlier observations,^{6–10,16} we found high levels of $EGFP^+$ cells that were primarily located in clusters throughout the infarcted tissue and in the bordering peri-infarct zone rather than in the viable myocardium. The analysis showed that all three BM-derived donor cell types survived and efficiently engrafted the infarcted myocardium.

It had been reported earlier that green autofluorescence can be mistaken for EGFP fluorescence in the ischemically injured

heart under epifluorescence illumination.¹⁷ TPLSM imaging of peri-infarct regions in Langendorff-perfused mouse hearts similarly revealed strongly autofluorescent structures. They could however be reliably distinguished from EGFP fluorescence on the basis of their distinct emission profiles under the vital imaging conditions used in this study (for details, see **Supplementary Data S1** and **Supplementary Figure S2**).

Engrafted donor-derived cells lack electrically evoked $[Ca^{2+}]_i$ transients

We next investigated the functional fate of $ACT\text{-EGFP}$ BM-derived cells after transplantation into peri-infarct regions. The hearts that had received LDM BM cells were examined first. The mice were killed 9 or 10 days after the BM cell injection, and the hearts were removed, loaded with rhod-2 (a calcium-sensitive fluorescent dye), and subjected to TPLSM imaging. Imaging was initially performed

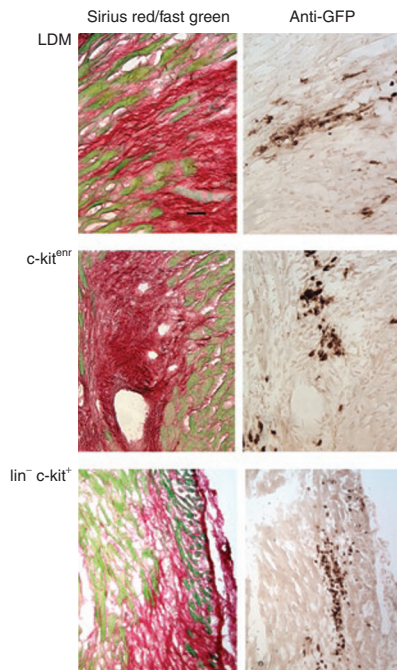


Figure 3 Direct transplantation and engraftment of *ACT-EGFP* bone marrow (BM) cells into infarcted myocardium of nontransgenic recipients. Left panels: Sirius red- and fast green-stained histological sections from infarcted hearts at 9 days after left coronary artery ligation and transplantation of 100,000 *ACT-EGFP* BM cells. Right panels: adjacent sections from the same hearts immunostained for EGFP (brown signal, horseradish peroxidase-conjugated secondary antibody, signal developed with diaminobenzidine reaction). Scale bar: 30 μ m. EGFP, enhanced green fluorescent protein; LDM, low-density mononuclear cells.

along the graft-host border, with the presence of $[Ca^{2+}]_i$ transients in host cardiomyocytes within the same microscopic field providing a good positive control. A representative frame-mode image obtained during remote point stimulation at 4 Hz is shown in **Figure 4a**. A cluster of small (<10 μ m diameter), round, donor-derived cells, readily identifiable by virtue of their EGFP fluorescence, were present adjacent to the peri-infarct border zone of the host myocardium. The host cardiomyocytes located on either side of the BM cell graft exhibited periodic increases in rhod-2 fluorescence (denoted by asterisks), reflecting cyclic increases in intracellular free calcium triggered by propagated action potentials. The calcium responses in these cells appear to be in synchrony and at the same frequency as remote stimulation, indicating that they are functionally coupled to the remote myocardium outside the peri-infarct region. In contrast, no $[Ca^{2+}]_i$ transients were detectable in the cluster of EGFP-expressing donor-derived cells.

We also obtained line-scan images from the graft-host border by repeatedly scanning at a high rate (500 Hz) along the white line in **Figure 4a** during remote electrical stimulation at 4 Hz. The scan line traversed a host cardiomyocyte, a juxtaposed capillary, and a small donor-derived cell. The line scans were then stacked such that the *y*-axis represents time and the *x*-axis represents distance (**Figure 4b**). Spatially averaged traces for the red and green fluorescence signals were then generated from the line-scan data (**Figure 4c**). These traces confirm the presence of action potential-evoked calcium responses in the host cardiomyocytes, and the absence of calcium responses in the neighboring LDM

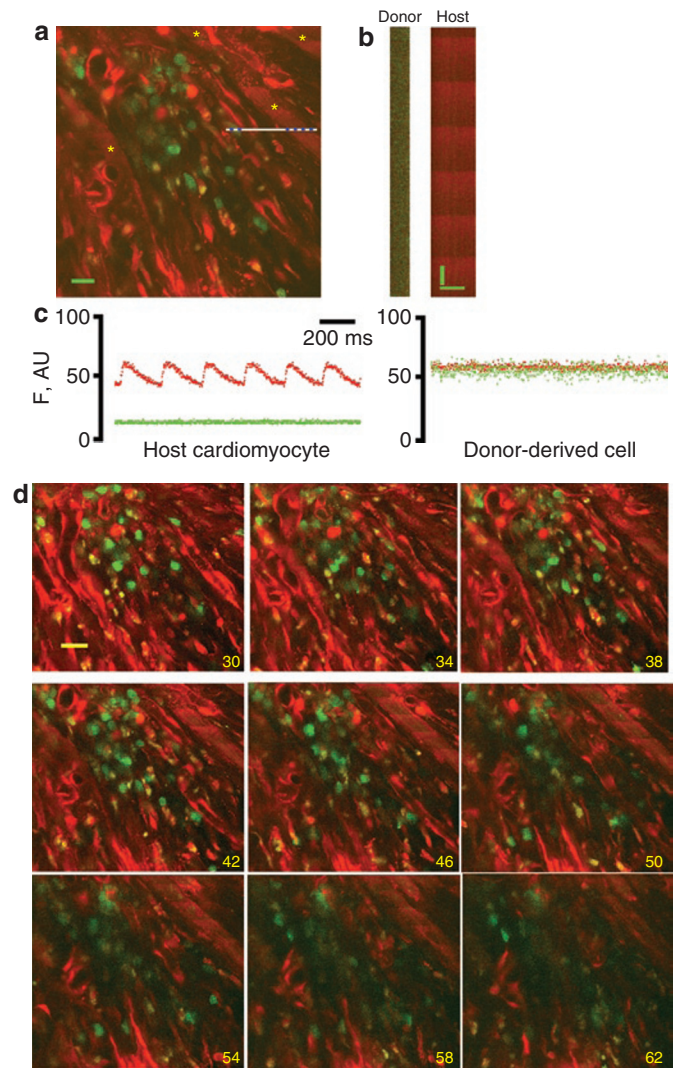


Figure 4 Simultaneous imaging of rhod-2 and enhanced green fluorescent protein (EGFP) fluorescence in a nontransgenic heart at 9 days after coronary artery ligation and injection of *ACT-EGFP* low-density mononuclear bone marrow cells into the peri-infarct zone. **(a)** Full-frame two-photon laser scanning fluorescence microscopy (TPLSM) image of the graft-host myocardium border zone. The hearts were loaded with rhod-2. Red (rhod-2) and green (EGFP) fluorescence signals were superimposed. Host cardiomyocytes and donor-derived cells (green/yellow) are apparent. The preparation was paced by point stimulation at a remote site at 4 Hz. The white bar demarcates the position of line-scan mode data acquisition. Asterisks denote host cardiomyocytes with $[Ca^{2+}]_i$ transients. Scale bar: 20 μ m. **(b)** Stacked line-scan images of the regions in **a** demarcated by the blue dotted lines. The line-scans traverse one non-EGFP-expressing (host) cardiomyocyte and one EGFP-expressing (donor derived) cell. Scale bars: 20 μ m horizontally, 125 ms vertically. **(c)** Spatially integrated changes in rhod-2 and EGFP fluorescence for one host cardiomyocyte and one juxtaposed donor-derived cell. The fluorescence signal across the entire cell was averaged. **(d)** Full-frame TPLSM images obtained from the heart depicted in **a** at increasing depths. The heart was paced by point stimulation at a remote site at 4 Hz. The numbers indicate nominal distance of the focal plane from the epicardial surface. Scale bar: 20 μ m.

BM-derived cells. A series of X, Y scans taken at 4- μ m *z*-steps along the graft-host border during continuous electrical point stimulation at 4 Hz similarly did not reveal calcium responses in the cluster of donor-derived cells (**Figure 4d**).

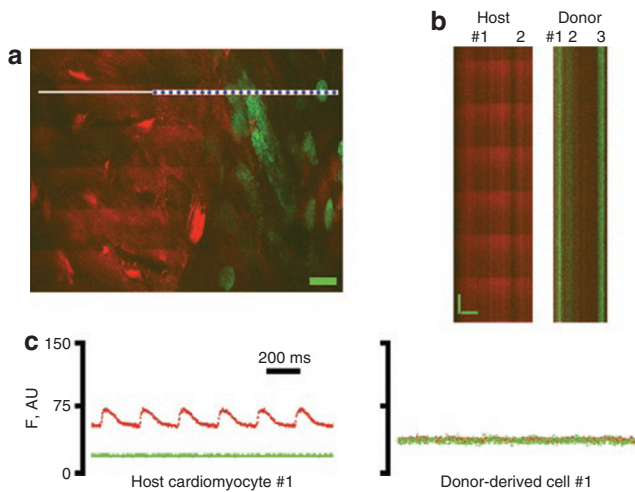


Figure 5 Simultaneous imaging of rhod-2 and enhanced green fluorescent protein (EGFP) fluorescence in a nontransgenic heart at 9 days following coronary artery ligation and injection of *ACT-EGFP c-kit^{enr}* bone marrow cells into the peri-infarct zone. **(a)** Full-frame two-photon laser scanning fluorescence microscopy image of the graft–host myocardium border zone. The hearts were loaded with rhod-2. Host cardiomyocytes (red) and donor-derived cells (green/yellow) are apparent. The preparation was paced by point stimulation at a remote site at 4 Hz. The white bar demarcates the position of line-scan mode data acquisition. Scale bar: 20 μ m. **(b)** Stacked line-scan images of the regions in **a** demarcated by the blue dotted lines. The line-scans traverse two non-EGFP-expressing (host) cardiomyocytes and three EGFP-expressing (donor derived) cells. Scale bars: 20 μ m horizontally, 125 ms vertically. **(c)** Spatially integrated changes in rhod-2 and EGFP fluorescence for one host cardiomyocyte and one juxtaposed donor-derived cell. The fluorescence signal across the entire cell was averaged. AU, arbitrary units; F, fluorescence.

In order to exclude the possibility that the absence of spontaneous and remote stimulation-evoked $[Ca^{2+}]_i$ transients in donor-derived cells results from a lack of electrical coupling between donor and host cells (rather than from an intrinsic inability to raise cytosolic calcium in response to membrane depolarization), we also monitored changes in $[Ca^{2+}]_i$ during electrical field stimulation (100 V, 2 ms, 3 Hz). Under these conditions, the development of $[Ca^{2+}]_i$ transients is no longer dependent on intercellular action potential propagation. Electrical field stimulation readily evoked $[Ca^{2+}]_i$ transients in host cardiomyocytes at sites remote from the graft as well as in areas bordering donor cell clusters, but not in donor-derived cells within the clusters. Collectively, these data indicate that engrafted LDM BM-derived cells within the infarcted tissue lack the ability to raise cytosolic calcium transiently in response to electrical membrane excitation. Similarly, no $[Ca^{2+}]_i$ transients were inducible in BM-derived cell clusters in the center of the scar during spontaneous sinus rhythm, remote electrical point stimulation, or electrical field stimulation. A total of >300 LDM BM-derived cells, imaged and distributed among eight animals, were shown to lack spontaneous or electrically evoked $[Ca^{2+}]_i$ transients.

We next examined the functional fate of *c-kit^{enr}* and *lin⁻c-kit⁺* BM cells following their direct injection into peri-infarct regions. Representative TPLSM images obtained from hearts 9 days after the transplantation of either donor cell type are shown **Figures 5** and **6**. Frame-mode and line-scan

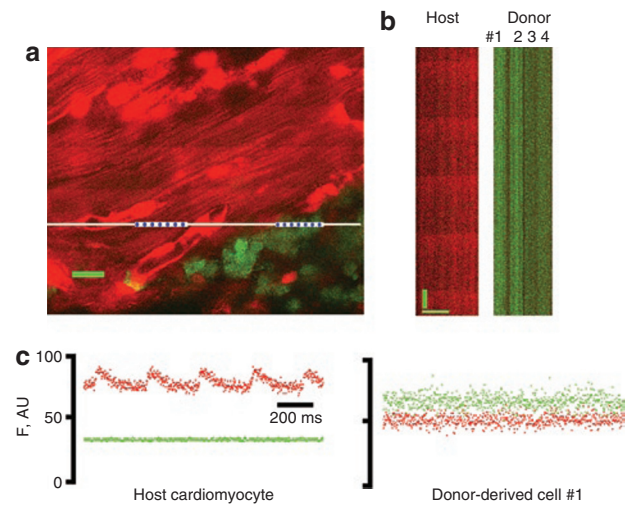


Figure 6 Simultaneous imaging of rhod-2 and enhanced green fluorescent protein (EGFP) fluorescence in a nontransgenic heart at 9 days after coronary artery ligation and injection of *ACT-EGFP lin⁻c-kit⁺* bone marrow (BM) cells into the peri-infarct zone. **(a)** Full-frame two-photon laser scanning fluorescence microscopy (TPLSM) image of the rhod-2-loaded heart at the graft–host border zone. The heart was continuously paced by point stimulation at a remote site at 3 Hz. Red (rhod-2) and green (EGFP) fluorescence signals were superimposed. Host cardiomyocytes (red) and donor-derived cells (green/yellow) are apparent. The white line demarcates the position of line-scan mode data acquisition. Scale bar: 20 μ m. **(b)** Line-scan mode images of the regions in **a** demarcated by the blue dotted lines. The line scans traverse one EGFP-negative (host) cardiomyocyte and four EGFP-expressing (donor derived) cells. Scale bars: 20 μ m horizontally, 125 ms vertically. **(c)** Spatially integrated changes in rhod-2 and EGFP fluorescence for one host cardiomyocyte and one donor-derived cell. The fluorescence signal across the entire cell was averaged. AU, arbitrary units; F, fluorescence.

mode images revealed synchronous and periodic increases in rhod-2 fluorescence in host cardiomyocytes at the graft–host border during electrical point stimulation at 4 Hz, but not in donor-derived cell clusters which, in many cases, appeared to be in physical contact with functioning host myocytes (see in **Figures 5a** and **6a**). Line scan data (**Figures 5b** and **6b**) were used for generating spatially averaged traces for the green and red fluorescent signals (**Figures 5c** and **6c**), which confirmed the presence of action potential-evoked $[Ca^{2+}]_i$ transients in host cardiomyocytes, and the absence of such transients in donor-derived cells, respectively. Electrical field stimulation also failed to evoke cytosolic calcium transients in these donor-derived cell populations. Moreover, we did not detect spontaneous or electrically evoked calcium responses in donor-derived cells located within the infarct scar remote from functioning host cardiomyocytes. Identical results were obtained in a total of >1,700 and >1,300 donor-derived cells after transplantation of *c-kit^{enr}* and *lin⁻c-kit⁺* BM cells, respectively. These cells were distributed among 10 animals per group. Therefore, our results indicate that the clustered EGFP-expressing cells, whether they are derived from LDM, *c-kit^{enr}*, or *lin⁻c-kit⁺* BM cells, lack the ability to develop cytosolic calcium transients in response to membrane depolarization, and consequently do not function as cardiomyocytes following direct transplantation into ischemically injured heart muscle.

Donor BM cells express hematopoietic lineage markers

Further evidence that the transplanted BM cells do not adopt a cardiomyocyte phenotype was obtained by immunohistological analyses. At 9 days after transplantation, immune staining revealed that clusters of EGFP-expressing cells, irrespective of the transplanted donor cell type, engrafted the infarct scar or infarct border zone (Figure 7a, d, and g), and expressed the pan-hematopoietic cell surface antigen CD45 (Figure 7b, e, and h), thereby suggesting differentiation into mature hematopoietic cells. Morphologically, CD45- and EGFP-double positive cells predominately exhibited a round shape, compatible with a hematopoietic phenotype (Figure 7c, f, and i). Occasionally, they had more elongated shapes reminiscent of the CD-45-positive fibroblast population recently described by Haudek *et al.*¹⁸ (Figure 7j and k). Moreover, immune staining with an anti- α -actinin antibody revealed that no EGFP-expressing cell exhibited sarcomeric structure. In contrast, sarcomeric structure was readily apparent in host cardiomyocytes (Figure 7l).

Limitations of the TPLSM imaging system

Accurate discrimination of donor cell rhod-2 fluorescence intensities from host cell fluorescence is crucial for arriving at an unambiguous finding regarding the functional state of individual donor cell-derived, EGFP-expressing cells *in situ*. All of the results presented above focused on the analysis of clusters of donor-derived cells, where interference from host cell rhod-2 fluorescence is not problematic. However, it was not clear whether the TPLSM system had sufficient resolution on the *z*-axis to discriminate between donor and host cell rhod-2 fluorescence when imaging isolated donor cells closely juxtaposed to host cardiomyocytes, particularly given the small size of the engrafted EGFP-expressing BM-derived cells. Preliminary control experiments to address this issue entailed image analysis of a non-engrafted, rhod-2 loaded, isolated perfused heart. Serial optical sections were recorded at 2.0- μ m axial intervals across a bifurcated capillary during continuous electrical point stimulation at a rate of 4 Hz. Action potential-induced rhod-2 transients were visible as ripple-like wave fronts which encompass the entire width of the field of view, even when the focal plane is moved into the capillary lumen (Figure 8a, arrows). *X, Z* reconstructions of the same capillary during continuous electrical stimulation confirmed the apparent presence of rhod-2 transients within the capillary lumen (Figure 8b, arrows). Identical observations were made in three more hearts. These findings indicate a degradation of spatial resolution at depth in living cardiac tissue under our imaging conditions. Measurements of the three-dimensional fluorescence profile of 1- μ m fluorescent spheres following intracoronary injection into a Langendorff-perfused heart revealed that a marked axial, but not lateral, broadening of the two-photon excitation volume underlies the decline of spatial resolution at depth (see Supplementary Data S1 and Supplementary Figure S3). Consequently, the apparent occurrence of rhod-2 transients within the capillary lumen (Figure 8a and b) reflects contamination from rhod-2 signals originating in cardiomyocytes both below and above the imaged capillary. Because we found that the axial dimension of a perfusate-filled capillary lumen in a Langendorff-perfused mouse heart is

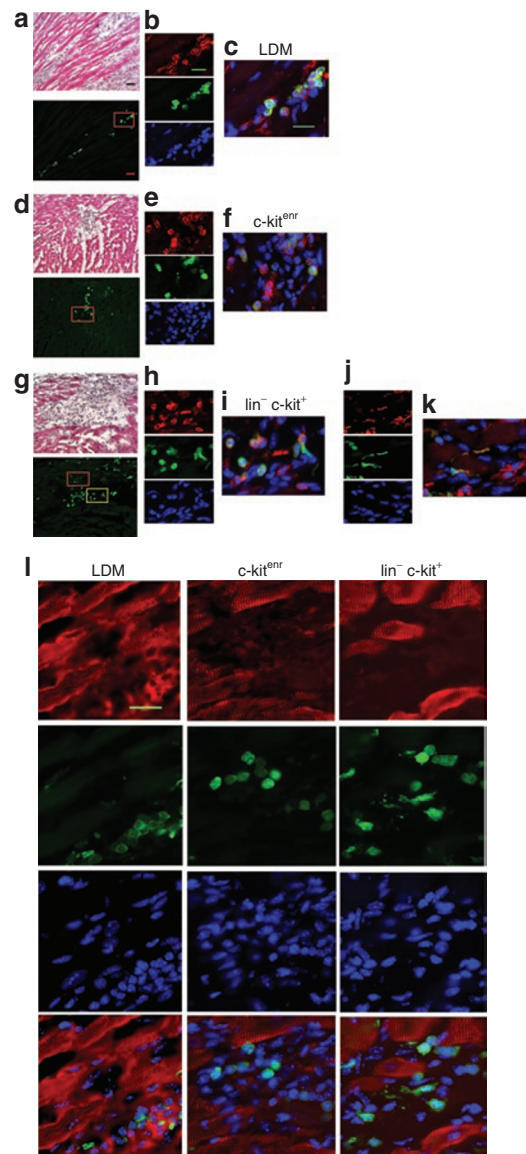


Figure 7 Immune histological analyses for CD45, enhanced green fluorescent protein (EGFP) and α -actinin in 10- μ m sections obtained from nontransgenic hearts at 9 days after coronary artery ligation and injection of (a–c) ACT-EGFP low-density mononuclear (LDM), (d–f) c-kit^{enr} or (g–k) lin⁻ c-kit⁺ bone marrow (BM) cells. The upper panels in a, d, and g show representative hematoxylin and eosin-stained sections of the transition zone between the surviving host myocardium and the infarct scar in the engrafted hearts. The lower panels show that the donor-derived cells (green) predominately engraft within scar tissue or at the infarct border zone, rather than within the viable myocardium. The upper panels in b, e, h, and j show representative images of CD45 expression, the middle panels show EGFP expression, and the lower panels show Hoechst nuclear staining; data is taken from the regions boxed in a, d, and g (panels h and j correspond to the yellow and red boxes, respectively, in g). Panels c, f, i, and k show the corresponding merged fluorescence images. Scale bar: 30 μ m in a; 20 μ m in b and c. (l) α -Actinin (red) expression, EGFP (green) expression and Hoechst nuclear staining in tissue sections adjacent to those shown in a, d, and g. Scale bar: 20 μ m.

typically 8–10 μ m (measured from *z*-stacks taken across capillaries as shown in Figure 8), we estimate that rhod-2 signals sampled from voxels located within at least a 5- μ m axial distance from a donor–host cell interface will represent variable contributions

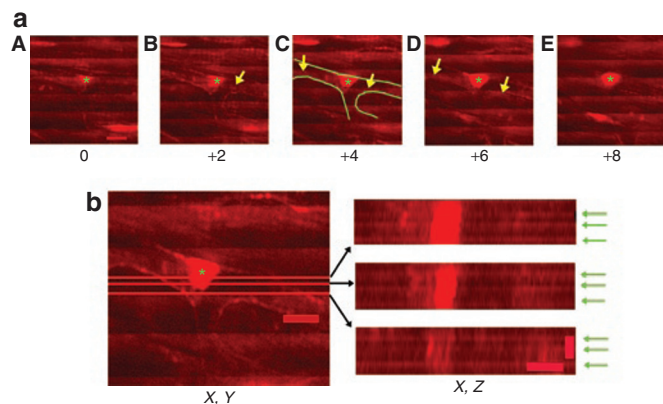


Figure 8 Spatial resolution of the imaging system in living heart tissue. **(a)** Series of X, Y scans obtained from an isolated perfused mouse heart loaded with rhod-2 using two-photon laser scanning fluorescence microscopy in nondescanned mode. Images were collected across a bifurcating capillary at 2- μm z -steps intervals during continuous electrical point stimulation at 4 Hz. Numbers indicate imaging depth (in μm) in reference to the image in **a**. The wave length of excitation light was 810 nm and rhod-2 fluorescence was collected between 560 and 650 nm. The green lines in **c** mark the capillary endothelium. Asterisks denote endothelial cell nuclei. Periodic increases in rhod-2 fluorescence resulting from action potential-evoked increases in cytosolic calcium concentration are visible as ripple-like wave fronts. Some X, Y scans reveal the appearance of cardiomyocyte-typical rhod-2 transients within the perfusate-filled capillary lumen (arrows). Scale bar: 10 μm . **(b)** Data sets shown in **a** were converted to a stack, and the stack was then resliced to obtain X, Z projections of the capillary. The red lines in the X, Y scan on the left indicate the X positions of the X, Z profiles shown on the right. The green arrows denote action potential-induced rhod-2 transients. In all three projections, rhod-2 transients are clearly detectable within the capillary lumen. Scale bars: 10 μm laterally, 5 μm axially.

from both cell types. Given this, and given the dimensions of the engrafted BM-derived EGFP expressing cells, the TPLSM imaging system cannot be used to screen for the presence of $[\text{Ca}^{2+}]_i$ transients in isolated donor cells when they are closely juxtaposed to host cardiomyocytes on the z -axis.

DISCUSSION

The data presented here confirm the ability of adult LDM, $c\text{-kit}^{\text{enr}}$, and $\text{lin}^- c\text{-kit}^+$ BM cells to engraft efficiently when directly injected into the hearts of mice that have been subjected to acute coronary artery ligation. In accordance with earlier observations,^{6–10,16} we found that the vast preponderance of donor-derived cells were located in clusters throughout the infarcted tissue and the bordering peri-infarct zone, 9 days after artery occlusion. TPLSM imaging revealed that, while spontaneous or remote point stimulation-evoked $[\text{Ca}^{2+}]_i$ transients were observed to occur synchronously in host cardiomyocytes along the graft–host border, they were absent in all imaged BM-derived cell clusters, irrespective of the donor cell type. Electrical field stimulation was equally ineffective in triggering $[\text{Ca}^{2+}]_i$ transients in these cells. Together, our results indicate that the imaged donor-derived cells within the infarct scar are electrically inexcitable and/or unable to raise cytosolic calcium transiently in response to membrane depolarization. This result is consistent with the complete absence of sarcomeric α -actinin immune reactivity, and the presence of CD45 immune reactivity, in the EGFP-expressing donor-derived cells.

Our data also show that the TPLSM imaging system has limits with regard to axial resolution. Previous calculations have predicted that two-photon fluorescence excitation (and thus emission) in tissue is confined to less than femtoliter volumes around the focal point of a 1.2-numerical aperture water immersion objective, with <1- μm resolution in the z direction.^{19–21} Wave-front aberrations caused by the refractive index structure of the specimen have been known to compromise three-dimensional resolution in multiphoton laser scanning fluorescence microscopy.^{22,23} Both theoretical and experimental approaches have shown that optical aberrations induced by refractive index mismatch cause a gradual decline in resolution (primarily in axial resolution) when attempting to image at increasing depths into living biological (*i.e.*, aqueous) specimens, even when water immersion objectives are used. In line with these observations, we found a significant axial broadening of the two-photon excitation volume with increasing distance of the focal plane from the epicardial surface of living, buffer-perfused mouse hearts, compromising the ability of our imaging system to properly discriminate donor cell derived from host cell-derived rhod-2 signals within an axial distance of several microns from the donor–host interface. Our attempts to enhance the axial resolution by introducing a pinhole in the detection path resulted in near-loss of the fluorescence signal at depth (data not shown), in accordance with earlier reports.²⁴

These physical constraints of the TPLSM imaging method preclude its ability to discriminate the origin of rhod-2 fluorescence signals in small donor cells when they are closely juxtaposed to host cardiomyocytes. Consequently, the system cannot be used to screen for the presence of functional attributes in isolated EGFP-expressing BM-derived cells that are located within a few microns from adjacent cardiomyocytes in the z -axis, given their small size. It is of interest to note that a TPLSM-based imaging approach was used in a recent study to demonstrate that some donor-derived cells apparently develop electrical stimulation-evoked rhod-2 transients in synchrony with host cardiomyocytes following engraftment into infarcted hearts.¹⁶ However, control experiments demonstrating sufficient *in situ* z -axis spatial resolution to discriminate between signals originating in donor and host cells under the experimental conditions employed were lacking. Given the z -axis signal deterioration reported by us and by others,^{22,23} it is highly possible that the rhod-2 transients observed in donor-derived cells in that study arose as a consequence of fluorescence contamination from juxtaposed host cardiomyocytes, and does not represent intrinsic cardiomyogenic activity in the donor cell.

Collectively, our results are incompatible with previous studies that had suggested that engrafted BM-derived cells exhibit both functional and structural characteristics of cardiomyocytes *in situ* (see Introduction). The underlying basis for this discrepancy is not clear. Given the simplicity of the isolation procedure, it is unlikely that the LDM BM cells used in this study differed from those in studies which reported cardiomyogenic activity.^{4,5} Our flow cytometry analyses, too, revealed that the scored attributes of the $c\text{-kit}^{\text{enr}}$ BM cells and $\text{lin}^- c\text{-kit}^+$ BM cells used in this study (Figure 2 and Supplementary Figure S1) appeared to be identical to those in the studies that reported cardiomyogenic activity.^{6,7} It is unlikely, therefore, that overt differences in the

cellular composition of donor cell populations can explain the discrepancies in study outcomes.

EGFP may selectively destroy a BM-derived cardiogenic precursor line; indeed, earlier studies have revealed that the protein could be cytotoxic.^{25,26} EGFP could also negatively interfere with cardiomyogenic activity. Alternatively, instability in EGFP fluorescence over time could give rise to a false negative result.⁸ Several observations argue against these explanations being valid. First, the surface antigen expression profile in EGFP-expressing c-kit^{enr} BM cell population was identical with that in the entire, EGFP-positive and -negative, c-kit^{enr} population (see **Supplementary Figure S1**). Second, adult *ACT-EGFP* cardiomyocytes stably express the fluorescent protein and function normally. Third, Orlic *et al.*⁶ found that the percentage of engrafted BM-derived *bona fide* myocytes co-expressing EGFP and cardiomyocyte-specific markers was similar to that of EGFP-expressing c-kit-positive cells before transplantation, thereby suggesting that EGFP does not negatively influence the transformation of BM cells into *bona fide* cardiomyocytes. It is therefore unlikely that the reporter gene negatively impacted cardiomyogenic activity in our study.

On the other hand, our results are in excellent agreement with those of a number of earlier studies that were conducted independently in different laboratories.^{8–10,27} These studies exclusively relied on molecular analyses to follow BM cell fate following transplantation (see Introduction). In this study, cross-checking the results of functional and immunohistological analyses provided additional strong evidence that engrafted adult LDM BM cells, c-kit^{enr} BM cells, and lin⁻ c-kit⁺ BM cells do not give rise to high levels of functionally competent cardiomyocytes following direct injection into hearts of mice subjected to acute myocardial infarction. These data suggest that any functional improvement seen in infarcted hearts receiving BM cell transplants, both in animal studies and clinical trials, is likely to reflect a beneficial effect imparted upon the surviving, pre-existing myocardium, rather than a direct contribution of electromechanically integrated BM-derived *de novo* cardiomyocytes. Possible mechanisms that underlie improvement in functional outcome following direct BM cell transplantation into ischemically injured myocardium appear to involve paracrine effects, resulting in prevention of cardiomyocyte apoptosis,²⁸ preservation of cardiomyocyte function,²⁸ and induction of angiogenesis.^{29,30}

MATERIALS AND METHODS

All the experiments reported in this study have been approved by the Institutional Review Board at the Indiana University School of Medicine.

Isolation of BM cells for intracardiac transplantation. BM was obtained from the tibias, femurs, and iliac crests of 6–8-week-old heterozygous C57BL/6-Tg(ACTB-EGFP)1Osb/J mice of either sex (Jackson Laboratories, Bar Harbor, ME). This transgenic mouse line (designated *ACT-EGFP*) ubiquitously expresses EGFP under the control of the chicken β -actin promoter and cytomegalovirus enhancer. Three different subsets of BM cells were collected for intracardiac transplantation:

i) Unfractionated LDM BM cells. The suspension of whole BM cells was overlaid with sodium metrizoate (Histopaque; Sigma, St. Louis, MI) solution (1.083 g/ml) and centrifuged at 740g for 25 minutes. The low-density cells were harvested, washed, and suspended (100,000 cells in 3 μ l phosphate-buffered saline) in preparation for intracardiac injection.

ii) c-kit-enriched (c-kit^{enr}) BM cells: LDM BM cells were reacted with a biotin-conjugated anti-mouse c-kit monoclonal antibody (clone ACK-4), and subsequently stained with streptavidin–phycoerythrin (streptavidin–PE) (Invitrogen, Carlsbad, CA). The ACK-4/biotin/streptavidin–PE-labeled cells were then incubated with anti-PE magnetic immunobeads (Miltenyi Biotec, Auburn, CA) and separated by magnet-activated cell sorting into c-kit⁺ and c-kit⁻ fractions. Cells expressing high levels of c-kit were used for intracardiac injection (c-kit^{enr} group).

iii) Lineage-depleted BM cells expressing high numbers of c-kit receptors (lin⁻ c-kit⁺ cells). LDM BM cells were incubated with a mixture of rat monoclonal antibodies directed against the following murine hematopoietic cell lineage-specific surface markers: B lymphocytes (B220), T lymphocytes (CD4 and CD8), granulocytes (Gr-1), myelomonocytic cells (Mac-1), and erythroid cells (Ter-119) (Pharmingen, San Diego, CA).¹⁵ Antibody-labeled lin⁺ cells were depleted using magnetic immunobeads (Miltenyi Biotec). The lineage-depleted cell population was then collected and incubated with a PE-conjugated anti-c-kit monoclonal antibody (clone ACK-4; Cedarlane Laboratories, Burlington, NC). Stained cells were sorted using a Becton-Dickinson cell sorter (Becton-Dickinson, Franklin Lakes, NJ), based on the number of c-kit receptors and levels of EGFP expression. Lin⁻ cells expressing high levels of both c-kit and EGFP were used for intracardiac transplantation (lin⁻ c-kit⁺ group).

Flow cytometry analyses of c-kit^{enr} BM cells. In a separate set of experiments, we determined the expression levels of various markers on the surfaces of *ACT-EGFP* c-kit^{enr} BM cells using flow cytometry. c-kit^{enr} BM cells were collected from heterozygous *ACT-EGFP* mice as described above. Because eluted cells were already reacted with CD117 that was developed by a PE-conjugated second step reagent, aliquots of these cells were stained with other markers for analysis, including PE-Cy5-conjugated sca-1, flk-1 allophycocyanin, a cocktail of allophycocyanin-conjugated lineage markers (CD3e, CD11b, CD45R/B220, Gr-1, and TER119), and biotinylated CD34 that was further developed with streptavidin-conjugated allophycocyanin-Cy7. Each aliquot was subsequently analyzed using flow cytometry to determine expression levels of these surface markers in the c-kit^{enr} cell population.

Coronary artery ligation and intracardiac grafting. Ten- to twelve-week-old, nontransgenic C57BL/6 mice were endotracheally intubated and ventilated with a rodent ventilator (Harvard Apparatus, Holliston, MA). Anesthesia was maintained with inhalational isoflurane. A thoracotomy was performed and an 8-0 polypropylene suture was placed around the distal left anterior descending coronary artery as described earlier.¹⁰ Donor cells (100,000) suspended in 3 μ l phosphate-buffered saline were injected into the anterior and posterior infarct border zones of the ischemic myocardium 3–5 hours after coronary ligation. The chest was closed and the animals were weaned from the ventilator and extubated.

Imaging of intracellular calcium transients using TPLSM. Imaging of intracellular calcium ([Ca²⁺]_i) transients in Langendorff-perfused hearts was performed as described earlier.^{11,12} The hearts of all the mice were subjected to TPLSM imaging at 9 or 10 days after intracardiac delivery of BM cells. Calcium responses in donor-derived cells and host cardiomyocytes were monitored during spontaneous sinus rhythm, electrical point stimulation at a site remote from the graft, and electrical field stimulation. For a more detailed description of the imaging approach see **Supplementary Data S1**.

Immunohistochemistry. The animals were killed and the hearts were removed 9 days after intracardiac injection of BM cells, washed in phosphate-buffered saline, immersed in fixation solution (1% paraformaldehyde and 1% cacodylic acid in phosphate-buffered saline) for 48 hours at 2–4°C, cryoprotected in 30% sucrose, and frozen in optimum cutting temperature compound. Ten-micrometer cryosections were obtained and stained for EGFP alone (rabbit anti-EGFP; Millipore, Billerica, MA) and

developed with diaminobenzidine, or were stained with an anti-CD45 primary antibody (rat anti-CD45; Pharmingen, San Diego, CA), visualized with an Alexa555-conjugated secondary antibody (Invitrogen, Carlsbad, CA) in combination with a fluorescein isothiocyanate-conjugated goat anti-GFP antibody (Novus Biologicals, Littleton, CO), and nuclear stained with 4,6-diamidino-2-phenylindole dihydrochloride (Invitrogen, Carlsbad, CA). Tissue α -actinin immune reactivity was detected with a mouse monoclonal antibody (Sigma, St. Louis, MI) and visualized using a rhodamine-conjugated secondary antibody (Millipore, Billerica, MA). Hematoxylin and eosin and sirius red/fast green stainings were carried out as described earlier.³¹

ACKNOWLEDGMENTS

The study was supported by the National Institutes of Health and the American Heart Association.

SUPPLEMENTARY MATERIAL

Figure S1. Expression levels of different surface markers in *ACT-EGFP* c-kit^{enr} cells expressing EGFP.

Figure S2. Differentiation of cellular autofluorescence from EGFP fluorescence in the infarct border zone.

Figure S3. Degradation of axial discrimination at depth in buffer-perfused mouse heart.

Data S1. Additional methods.

REFERENCES

- Rubart, M and Field, LJ (2006). Cardiac regeneration: repopulating the heart. *Annu Rev Physiol* **68**: 29–49.
- Bittner, RE, Schöfer, C, Weipoltshammer, K, Ivanova, S, Streubel, B, Hauser, E *et al.* (1999). Recruitment of bone-marrow-derived cells by skeletal and cardiac muscle in adult dystrophic mdx mice. *Anat Embryol (Berl)* **199**: 391–396.
- Jackson, KA, Majka, SM, Wang, H, Pocius, J, Hartley, CJ, Majesky, MW *et al.* (2001). Regeneration of ischemic cardiac muscle and vascular endothelium by adult stem cells. *J Clin Invest* **107**: 1395–1402.
- Xaymardan, M, Tang, L, Zagreda, L, Pallante, B, Zheng, J, Chazen, JL *et al.* (2004). Platelet-derived growth factor-AB promotes the generation of adult bone marrow-derived cardiac myocytes. *Circ Res* **94**: E39–E45.
- Fernández-Avilés, F, San Román, JA, García-Frade, J, Fernández, ME, Peñarrubia, MJ, de la Fuente, L *et al.* (2004). Experimental and clinical regenerative capability of human bone marrow cells after myocardial infarction. *Circ Res* **95**: 742–748.
- Orlic, D, Kajstura, J, Chimenti, S, Jakoniuk, I, Anderson, SM, Li, B *et al.* (2001). Bone marrow cells regenerate infarcted myocardium. *Nature* **410**: 701–705.
- Kajstura, J, Rota, M, Whang, B, Cascapera, S, Hosoda, T and Bearzi, C (2005). Bone marrow cells differentiate in cardiac cell lineages after infarction independently of cell fusion. *Circ Res* **96**: 127–137.
- Balsam, LB, Wagers, AJ, Christensen, JL, Kofidis, T, Weissman, IL and Robbins, RC (2004). Haematopoietic stem cells adopt mature haematopoietic fates in ischaemic myocardium. *Nature* **428**: 668–673.
- Nygren, JM, Jovinge, S, Breitbach, M, Säwén, P, Röhl, W, Hescheler, J *et al.* (2004). Bone marrow-derived hematopoietic cells generate cardiomyocytes at a low frequency through cell fusion, but not transdifferentiation. *Nat Med* **10**: 494–501.
- Murry, CE, Soonpaa, MH, Reinecke, H, Nakajima, H, Nakajima, HO, Rubart, M *et al.* (2004). Haematopoietic stem cells do not transdifferentiate into cardiac myocytes in myocardial infarcts. *Nature* **428**: 664–668.
- Rubart, M, Wang, E, Dunn, KW and Field, LJ (2003). Two-photon molecular excitation imaging of Ca²⁺ transients in Langendorff-perfused mouse hearts. *Am J Physiol Cell Physiol* **284**: C1654–C1668.
- Rubart, M, Pasumarthi, KB, Nakajima, H, Soonpaa, MH, Nakajima, HO and Field, LJ (2003). Physiological coupling of donor and host cardiomyocytes after cellular transplantation. *Circ Res* **92**: 1217–1224.
- Okabe, M, Ikawa, M, Kominami, K, Nakanishi, T and Nishimune, Y (1997). “Green mice” as a source of ubiquitous green cells. *FEBS Lett* **407**: 313–319.
- Orlic, D, Kajstura, J, Chimenti, S, Bodine, DM, Leri, A and Anversa, P (2001). Transplanted adult bone marrow cells repair myocardial infarcts in mice. *Ann NY Acad Sci* **938**: 221–229; discussion 229–230.
- Orlic, D, Fischer, R, Nishikawa, S, Nienhuis, AW and Bodine, DM (1993). Purification and characterization of heterogeneous pluripotent hematopoietic stem cell populations expressing high levels of c-kit receptor. *Blood* **82**: 762–770.
- Rota, M, Kajstura, J, Hosoda, T, Bearzi, C, Vitale, S, Esposito, G *et al.* (2007). Bone marrow cells adopt the cardiomyogenic fate *in vivo*. *Proc Natl Acad Sci USA* **104**: 17783–17788.
- Lafamme, MA and Murry, CE (2005). Regenerating the heart. *Nat Biotechnol* **23**: 845–856.
- Haudek, SB, Xia, Y, Huebener, P, Lee, JM, Carlson, S, Crawford, JR *et al.* (2006). Bone marrow-derived fibroblast precursors mediate ischemic cardiomyopathy in mice. *Proc Natl Acad Sci USA* **103**: 18284–18289.
- Rubart, M (2004). Two-photon microscopy of cells and tissue. *Circ Res* **95**: 1154–1166.
- Helmchen, F, Svoboda, K, Denk, W and Tank, DW (1999). *In vivo* dendritic calcium dynamics in deep-layer cortical pyramidal neurons. *Nat Neurosci* **2**: 989–996.
- Brown, EB, Shear, JB, Adams, SR, Tsiens, RY and Webb, WW (1999). Photolysis of caged calcium in femtoliter volumes using two-photon excitation. *Biophys J* **76**: 489–499.
- Booth, MJ and Wilson, T (2001). Refractive-index-mismatch induced aberrations in single-photon and two-photon microscopy and the use of aberration correction. *J Biomed Opt* **6**: 266–272.
- Niesner, R, Andresen, V, Neumann, J, Spiecker, H and Gunzer, M (2007) The power of single and multibeam two-photon microscopy for high-resolution and high-speed deep tissue and intravital imaging. *Biophys J* **93**: 2519–2529.
- Gauderon, R, Lukins, PB and Sheppard, CJ (1999). Effect of a confocal pinhole in two-photon microscopy. *Microsc Res Tech* **47**: 210–214.
- Huang, WY, Aramburu, J, Douglas, PS and Izumo, S (2000). Transgenic expression of green fluorescence protein can cause dilated cardiomyopathy. *Nat Med* **6**: 482–483.
- Agbulut, O, Coirault, C, Niederländer, N, Huet, A, Vicart, P, Hagège, A *et al.* (2006). GFP expression in muscle cells impairs actin-myosin interactions: implications for cell therapy. *Nat Methods* **3**: 331.
- Deten, A, Volz, HC, Clamors, S, Leiblein, S, Briest, W, Marx, G *et al.* (2005). Hematopoietic stem cells do not repair the infarcted mouse heart. *Cardiovasc Res* **65**: 52–63.
- Uemura, R, Xu, M, Ahmad, N and Ashraf, M (2006). Bone marrow stem cells prevent left ventricular remodeling of ischemic heart through paracrine signaling. *Circ Res* **98**: 1414–1421.
- Kamihata, H, Matsubara, H, Nishiue, T, Fujiyama, S, Tsutsumi, Y, Ozono, R *et al.* (2001). Implantation of bone marrow mononuclear cells into ischemic myocardium enhances collateral perfusion and regional function via side supply of angioblasts, angiogenic ligands, and cytokines. *Circulation* **104**: 1046–1052.
- Fazel, S, Cimini, M, Chen, L, Li, S, Angoulvant, D, Fedak, P *et al.* (2006). Cardioprotective c-kit⁺ cells are from the bone marrow and regulate the myocardial balance of angiogenic cytokines. *J Clin Invest* **116**: 1865–1877.
- Nakajima, H, Nakajima, HO, Dembowsky, K, Pasumarthi, KB and Field, LJ (2006). Cardiomyocyte cell cycle activation ameliorates fibrosis in the atrium. *Circ Res* **98**: 141–148.